

## Velocity-Selective Magnetization-Prepared Non-Contrast-Enhanced Cerebral MR Angiography at 3T

Qin Qin<sup>1,2</sup>, Taehoon Shin<sup>3</sup>, Michael Schar<sup>1</sup>, Hua Guo<sup>4</sup>, and Ye Qiao<sup>1</sup>

<sup>1</sup>Radiology, Johns Hopkins University, Baltimore, Maryland, United States, <sup>2</sup>Kirby Center, Kennedy Krieger Institute, Baltimore, Maryland, United States, <sup>3</sup>Radiology, University of Maryland, Baltimore, Maryland, United States, <sup>4</sup>Center for Biomedical Imaging Research, Biomedical Engineering, Tsinghua University, Beijing, China

**TARGET AUDIENCE:** MRI physicists and clinicians interested in non-contrast-enhanced cerebral angiography.

**PURPOSE:** Among many non-contrast-enhanced MR angiography (NCE-MRA) techniques, the recently introduced velocity-selective saturation (VSS) pulse train (flowing spins in the pass-band with static tissues in the saturation-band)<sup>1</sup> allows for a large volume coverage within a single scan. Using the excitation  $k$ -space formalism<sup>2,3</sup>, the VSS pulse train with embedded refocusing pulses can reduce off-resonance effects and was first developed for peripheral MRA at 1.5T<sup>1</sup>. We have since reported an extended velocity-selective inversion (VSI) pulse train designed with more robust insensitivity to B0/B1 field inhomogeneity and applied it for cerebral blood flow mapping using arterial spin labeling approach at 3T<sup>4</sup>. Here we demonstrate the VSS magnetization-prepared cerebral MRA at 3T.

**METHODS:** To better combat B0/B1 inhomogeneity for the VSS pulse, paired composite refocusing pulses are inserted for each  $k$ -segment with phase cycling applied over consecutive  $k$ -segments (Fig. 1)<sup>4</sup>. Flow-sensitivity is achieved by alternating the polarities of the gradient (z-direction). Varying gradient strengths can encode velocity with different saturation bands and field of speed (FOS). In this study, two gradient strength conditions were compared including 1) saturation band within  $\pm 6$ cm/s and FOS=30cm/s (Fig. 1); and 2) saturation band within  $\pm 12$ cm/s and FOS=60cm/s. Both 32ms (Fig.1) and 53ms pulse train durations (less eddy-current effect) were tested (3T Philips, 32-channel head-receive coil, five healthy subjects with informed consent). First, an axial slab of 45mm thickness (0.7mm isotropic) around the Circle of Willis was imaged. 3D turbo field echo image acquisition: TR/TE=10/5.8ms, flip angle=6°, TFE factor=90, TFE acquisition window=927 ms, TFE shot interval=2000ms, SENSE 3x1, 2min. With the same resolution and volume coverage, the images were compared with a Time of Flight (TOF) scan (TR/TE=23/3.5ms, flip angle=18°, SENSE 3x1, 3min). Then the VSS prepared MRA was repeated for the whole-brain coverage with sagittal orientation (SENSE 3x2, 4.5min). To remove the interference of the surrounding tissues (fat, skull, muscle, etc), the brain was manually extracted from the raw images before MIP.

**RESULTS AND DISCUSSION:** The simulated Mz-velocity response of the VSS pulse train to velocities is displayed in Fig. 2, with overall velocity-selective profile maintained for a range of B0/B1 offset incurred in the brain area at 3T. Note that the saturation bands are still affected by the B1 field due to the hard pulses for  $k$ -space weighting. Fig. 3 compares the MIP images of the Circle of Willis: gradient strength 1) with the pulse duration of (a) 53ms and (b) 32ms; (c) TOF; gradient strength 2) with the pulse duration of (d) 53ms; (e) 32ms; (f) velocity-compensated counterpart of (b). Smaller VSS saturation band can have better depicting of the vessels with the slower flow, such as the small branches of the MCA and PCA, Fig. 3 (a) vs. (d), (b) vs. (e) (arrows). Longer VSS pulse duration leads to lower signal of the blood due to  $T_2$  relaxation and also higher chances of blood velocity variation during the pulse (such as pulsation or blood vessel tortuosity), Fig. 3 (a) vs. (b), (d) vs. (e). Compared to TOF, VSS prepared MRA depicts more distal MCA and PCAs with slower flow at more parallel flowing directions to the axial slab, Fig. 3 (b) vs. (c). The images of the same VSS pulse train except using velocity-sensitive and velocity-compensated gradient waveforms, demonstrate directly the velocity-selective utility of the preparation pulse train, Fig. 3 (b) vs. (f). Fig. 4 exhibits the sagittal (a) and coronal (b) MIP of the VSS prepared (gradient strength 1, 32ms) MRA of the whole brain. Both major arteries (ICA, VA, BA, MCA, ACA, PCA) and their small branches, and major veins (IJV, TS, SS) are depicted. Static tissue background is nicely suppressed in the center of the cranium and less saturated at the cortex and neck region, due to the B1 inhomogeneity distribution in the brain.

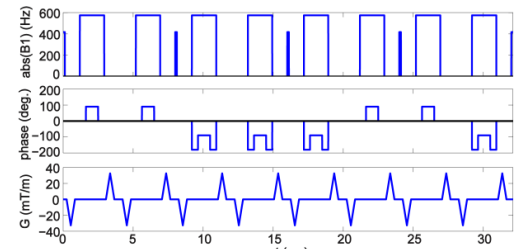


Fig.1: Velocity-selective saturation (VSS) pulse train a saturation band within  $\pm 6$ cm/s and a FOS=30cm/s.

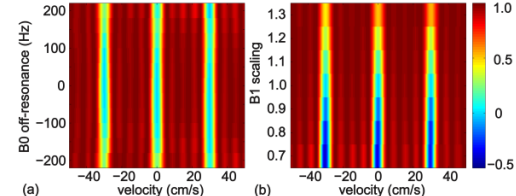


Fig.2: The simulated Mz-Velocity responses at different (a) B0 and (b) B1 conditions for the described VSS pulse train with inserted dual composite refocusing pulses.

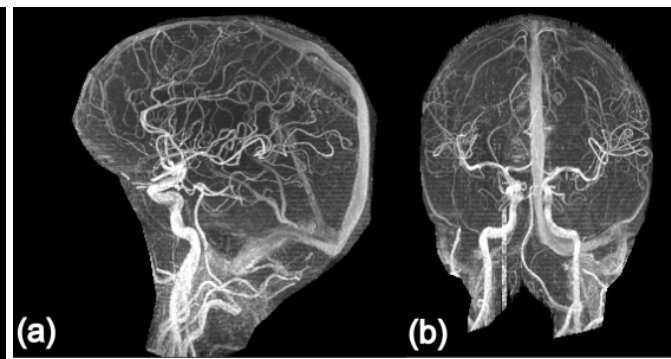
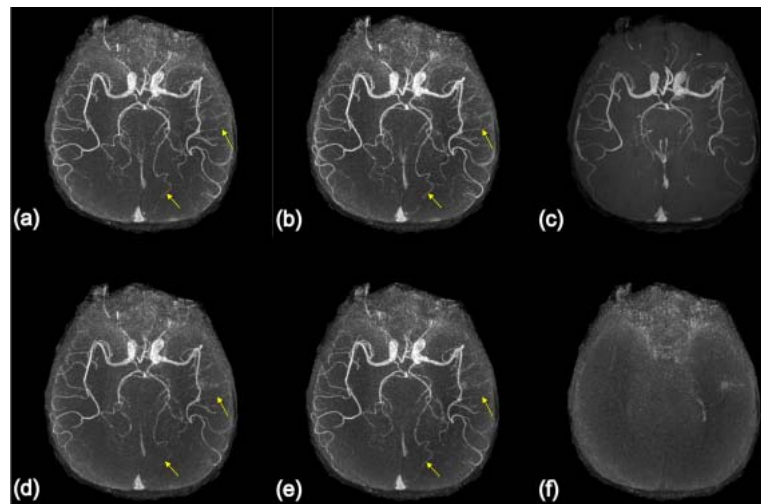


Fig.3: Axial MIPs: VSS saturation band=6cm/s with FOS=30cm/s: (a) 53ms; (b) 32ms; (c) TOF; VSS saturation band=12cm/s with FOS=60cm/s: (d) 53ms; (e) 32ms; (f) velocity-compensated counterpart of (b).

Fig.4: The sagittal (a) and coronal (b) MIPs of the VSS prepared MRA of the whole brain acquired with sagittal orientation.

**CONCLUSION:** We have developed the VSS prepared cerebral MRA at 3T, based on the improved robustness to B0/B1 field inhomogeneity for  $k$ -space based VS pulse trains. Compared with TOF MRA, VSS prepared MRA depicted more distal branches of cerebral arteries and allowed for the whole-brain coverage without the requirement of section positioning orthogonal to the direction of flow. The proposed technique will be further improved to have more uniform saturation band under different B1 offset. Strategies to better suppress fat and vein signals are currently under investigation.

**REFERENCE:** 1. Shin T, et al. *MRM* 2013(70):1229; 2. de Rochefort L, et al. *MRM* 2006(55):171; 3. Shin T, et al. *MRM* 2013(69):1268; 4. Qin Q, et al. *ISMRM* 2014:420;

**FUNDING SOURCE:** NIH K25 HL121192 (QQ) and NIH R00HL106232 (YQ)